Article

Optical Absorption of the Blue Fluorescent Protein: A First-Principles Study

Xabier Lopez, Miguel A. L. Marques, Alberto Castro, and Angel Rubio

J. Am. Chem. Soc., **2005**, 127 (35), 12329-12337• DOI: 10.1021/ja050935l • Publication Date (Web): 16 August 2005

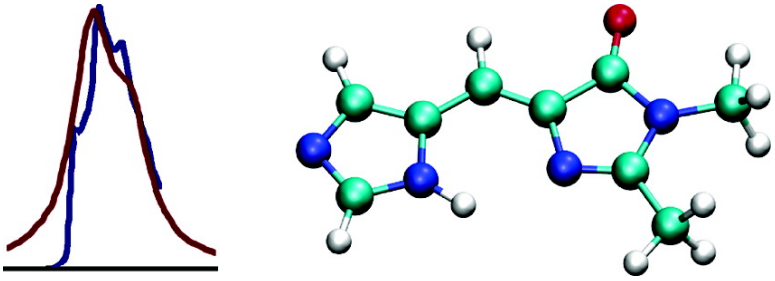

J|A|C|S
ARTICLES
Published on Web 08/16/2005

Optical Absorption of the Blue Fluorescent Protein: A First-Principles Study

Xabier Lopez,*[,†,‡] Miguel A. L. Marques,[§,¶] Alberto Castro,[§] and Angel Rubio[‡¶]

Contribution from the Kimika Fakultatea, Euskal Herriko Unibertsitatea, 20080 Donostia, Spain, Donostia International Physics Center (DIPC), E20018 Donostia/San Sebastián, Spain, Institut für Theoretische Physik, Freie Universität Berlin, Arnimallee 14, 14195 Berlin, Germany, and Departamento de Física de Materiales, Facultad de Ciencias Químicas, UPV/EHU and Unidad de Materiales Centro Mixto CSIC-UPV/EHU San Sebastián, Spain

Received February 14, 2005; E-mail: poplopex@sq.ehu.es; marques@teor.fis.uc.pt; alberto@physik.fu-berlin.de; arubio@sc.ehu.es

Abstract: An extensive study of the optical absorption spectra of the blue fluorescent protein (BFP) is presented. We investigate different protonation states of the chromophore (neutral, anionic, and cationic) and analyze the role of the protein environment and of thermal fluctuations. The role of the environment is 2-fold: (i) it induces structural modifications of the gas-phase chromophore, the most important being the torsion of the imida rings; and (ii) it makes a local-field modification of the external electromagnetic field. It turns out that the torsion of the imida rings shifts significantly the gas-phase spectra to lower energies, whereas the consistent inclusion of the closest residues field produces only minor modifications on the spectra. From all of the configurations studied, the neutral cis-HSD and the anionic HSA seem to be the most likely candidates to explain the experimental spectrum. Furthermore, the present results clearly rule out the presence of the cationic protonation state (HSP) of the chromophore. However, a better description of the measured experimental absorption data may be obtained when the temperature fluctuations of the floppy torsional motion of the two imida rings are included. Our results, together with previous work on the green fluorescent protein, demonstrate the power of combining time-dependent density functional calculations and optical absorption measurements to discern the relevant chemical information on the nature and state of chromopeptides.

I. Introduction

The study of the optical properties of biochromophores has developed into an important and active field of research. The rationale is clear, as the absorption and emission of light by biomolecules are at the center of crucial biophysical processes, such as vision or photosynthesis, and has led to various important technological applications. Among photoactive proteins, and due to its unique photophysical properties,[1] the family composed by the green fluorescent protein (GFP) and its mutants has attracted a considerable amount of attention during the past decade. These molecules have been used as important and versatile fluorescent markers, with widespread applications in the field of biotechnology. One of the originalities of the GFP resides in the fact that the chromophore responsible for the photophysics of the protein, 4-*p*-hydroxybenzylideneimidazolidin-5-one, is completely generated by an autocatalytic, post-translational cyclization and oxidation of the −Ser66−Tyr66−Gly67− triad, without the need of any external cofactor. Thus, all of the information needed to synthesize the biochromophore is encoded in the corresponding gene. Furthermore, the GFP can be easily attached to other proteins without changing its own absorption properties. This unique characteristic, due to the protective cage-like secondary structure of the protein, makes the GFP an ideal candidate for a biological marker.

With the widespread use of the GFP, there has been an increasing demand for the ability to visualize different proteins in vivo that require multicolor mode imaging.[2] This has triggered intensive research aimed at the development of GFP mutant forms with different optical responses. A mutant of the chromophore of particular interest is the Y66H variant, in which Tyr66 is mutated to His.[3,4] The resultant protein exhibits fluorescence shifted to the blue range and is, for that reason, often referred to as the blue emission variant of the GFP, or the blue fluorescent protein (BFP; see Figure 1).

Important differences and similarities exist in the absorption spectra of the GFP and BFP. The optical absorption spectrum[4−7] of the wild-type (wt) GFP has two main resonances at 2.63 and 3.05 eV, which are normally attributed to two protonation states

[†] Euskal Herriko Unibertsitatea.
[‡] DIPC.
[§] Freie Universität Berlin.
[¶] UPV/EHU.

(1) Zimmer, M. *Chem. Rev.* **2002**, *102*, 759−781 and references therein.
(2) Heim, R.; Tsien, R. *Curr. Biol.* **1996**, *6*, 178−182.
(3) Wachter, R.; King, B.; Heim, R.; Kallio, K.; Tsien, R.; Boxer, S.; Remington, S. *Biochemistry* **1997**, *36*, 9759−9765.
(4) Bublitz, G.; King, B.; Boxer, S. *J. Am. Chem. Soc.* **1998**, *120*, 9370−9371.
(5) Yang, F.; Moss, L. G.; Phillips, G. N., Jr. *Nat. Biotechnol.* **1996**, *14*, 1246−1252.
(6) Chattoraj, M.; King, B.; Bublitz, G.; Boxer, S. *Proc. Natl. Acad. Sci. U.S.A.* **1996**, *93*, 8362−8367.
(7) Niwa, H.; Inouye, S.; Hirano, T.; Matsuno, T.; Kojima, S.; Kubota, M.; Ohashi, M.; Tsuji, F. *Proc. Natl. Acad. Sci. U.S.A.* **1996**, *93*, 13617−13622.

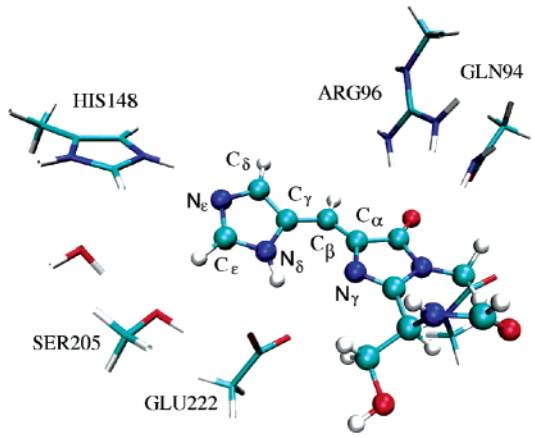

Figure 1. Structure of the cis-HSD chromophore (balls and sticks) of the blue fluorescent protein and of its closest residues. We also indicate the nomenclature used in the text for each atom. In the QM/MM calculations, the QM region is defined as the chromophore atoms shown in ball-and-sticks plus H-link atoms for the QM/MM boundaries. In the case of the TDDFT calculations, some residues around the chromopeptide were added to the QM part. Thus, His148, Glu222, and Arg96 form *Environment I*, whereas His148, Glu222, Arg96, Ser205, Gln94, and the water molecule (all residues shown in the figure) form *Environment II*.

of the chromophore.[8] These two states, one anionic and the other neutral, result from the deprotonation/protonation of Tyr66. On the other hand, the spectrum of the BFP (see Figure 5) is characterized by absorption between 3 and 3.5 eV, with a main peak appearing at 3.21 eV and a secondary peak at 3.36 eV. Furthermore, the spectrum also shows a smaller peak at 3.05 eV and finally a shoulder at 3.49 eV. Another important characteristic of the spectrum is the shift observed between folded and unfolded conformations of the BFP protein. According to Wachter et al.,[3] the excitation spectrum of the BFP chromophore in the folded protein exhibits an absorbance maximum at 3.25 eV. However, in the unfolded protein, the absorbance maximum is at 3.38 eV. Thus, the observed effect of the protein folding is a red-shift in absorbance of about 0.13 eV. Comparing this spectrum with the one of the wt-GFP, we observe that the BFP absorbs in the region corresponding to the neutral state of the GFP. However, the low-energy peak detected at 2.63 eV in the GFP (corresponding to the anionic state of the chromophore) is not present in the BFP.

In the case of the BFP, the assignment of the absorption peaks to specific protonation states is a difficult task. In principle, the 4-imidazoleimidazolidin-5-one chromophore of the BFP can assume three different protonation states (cationic, neutral, and anionic), in several possible conformations (see Figure 2). Estimations of the pK_a of the chromopeptide[3] points to values of 4 and 13 for pK_a^1 and pK_a^2, respectively, which seems to exclude a significant population of the anionic state of the BFP in the ground state. Nevertheless, the anionic state could, in principle, be formed in the excited state, as in the case of the wt-GFP.[1] If this is the case, it is likely that this state has a very short lifetime since a proton transfer from the protonated His148 would again neutralize the chromophore.

Recently, we demonstrated how a QM/MM molecular dynamics characterization of the chromophore structure in the protein matrix and first-principles time-dependent density functional theory (TDDFT) calculations can be combined to obtain useful chemical information on the nature and state of biochromophores.[8] QM/MM combines the ability of molecular mechanics to efficiently simulate very large compounds and the necessity of quantum mechanics to compute many important quantities and to model chemical reactions. It is currently the method of choice to study the dynamics of chromophores embedded in large protein matrices. On the other hand, TDDFT is a very powerful tool for the calculation of excitation spectra of finite systems. It has, therefore, become a popular method to solve this kind of problems both in physics (atomic, molecular, and condensed matter) and in quantum chemistry.[9−13]

In this work, we apply our combined approach QM/MM−TDDFT to the calculation of the optical absorption spectrum of the different protonation states and conformers of the BFP. Our results indicate that the most likely protonation state of the BFP is the neutral (HSD in Figure 2). Furthermore, the influence of the protein environment in the absorption spectrum is mainly of structural origin, by inducing a distorted nonplanar structure in the chromopeptide. This could be contributing to the observed red-shift in the absorption spectrum when the protein is folded. However, a better agreement with the measured experimental absorption data may be obtained when the temperature fluctuations of the floppy torsional motion of the two imida rings are included.

This article is organized as follows. In the next section, we describe our methods. These include (i) ground-state density functional calculations of the chromophore in the gas phase; (ii) QM/MM techniques to characterize the structure of the chromophore under the influence of the protein matrix; and (iii) TDDFT to obtain the absorption spectra. The following section is devoted to the presentation and discussion of our results. We start by studying the structure, energetics, and optical spectra of the chromopeptide in the gas phase. Next, we investigate the influence of the protein matrix, the role of the charged residues closest to the chromophore, and the effect of temperature on the spectra. Finally, we draw our conclusions and give a small overview.

II. Methods

A. Density Functional Calculations in the Gas Phase. The structures of the different protonation states and conformations of the chromophore were characterized in the gas phase. The combination of four different protonation states (one cationic, two neutrals, and one anionic) and three structures for each (two stable structures, and one transition state) leads to 12 different conformations, which are depicted in Figure 2.

All calculations were carried out using the Gaussian 98 suite of programs.[14] The gas-phase structures were optimized at the B3LYP/6-31++G(d,p) level,[15−18] and the electronic energy was then refined,

(8) Marques, M. A. L.; Lopez, X.; Varsano, D.; Castro, A.; Rubio, A. *Phys. Rev. Lett.* **2003**, *90*, 258101.
(9) Gross, E. K. U.; Dobson, J. F.; Petersilka, M. In *Density Functional Theory II, Topics in Current Chemistry*; Nalewajski, R., Ed.; Springer: Berlin, 1996; Vol. 181, pp 81−172.
(10) Casida, M. E. In *Recent Developments and Applications of Modern Density Functional Theory*; Seminario, J. M., Ed.; Elsevier Science: Amsterdam, 1996; pp 391−439.
(11) Marques, M. A. L.; Gross, E. K. U. *Annu. Rev. Phys. Chem.* **2004**, *55*, 427−455.
(12) Marques, M. A. L.; Gross, E. K. U. In *A Primer in Density Functional Theory*; Fiolhais, C., Nogueira, F., Marques, M. A. L., Eds.; Springer-Verlag: Berlin, 2003; pp 144−184.
(13) Onida, R.; Reining, L.; Rubio, A. *Rev. Mod. Phys.* **2002**, *74*, 601−659.
(14) Frisch, M. J. et al. *Gaussian 98*, revision a.2; Gaussian, Inc.: Pittsburgh, PA, 1998.
(15) Vosko, S. H.; Wilk, L.; Nusair, M. *Can. J. Phys.* **1980**, *58*, 1200−1211.
(16) Becke, A. *Phys. Rev. A* **1988**, *38*, 3098−3100.
(17) Lee, C.; Yang, W.; Parr, R. *Phys. Rev. B* **1988**, *37*, 785−789.

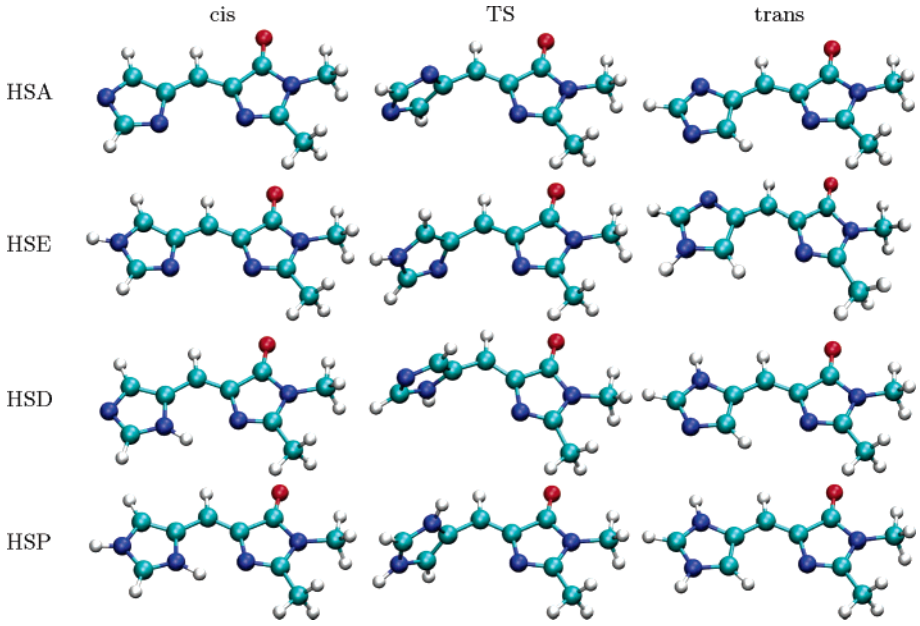

Figure 2. All gas-phase structures of the BFP chromophores characterized in the present work: the various protonation states, including the cis/trans conformations and the transition state configuration.

at optimized geometries, by single-point calculations at the B3LYP/6-311++G(3df,2p) level. The enthalpic and entropic corrections were determined with a frequency calculation at the B3LYP/6-31++G(d,p) level.[19] These frequencies were also used to verify the nature of the stationary points encountered. Thus, reactants, intermediates, and products exhibited real frequencies for all normal modes of vibration, whereas the transition states showed one imaginary frequency for the normal mode along the cis−trans isomerization. The free energy was obtained as a sum of the B3LYP/6-311++G(d,p) energy, the zero-point vibrational energy (ZPVE), the vibrational correction to the ZPVE at 298 K, and the rotational and translational energies at 298 K. The zero-point vibrational energy and the thermal vibrational energy were calculated in the rigid rotor-harmonic oscillator approximation. The rotational and translational energies were treated classically as 1/2 *RT* per degree of freedom.

The nomenclature of the atoms in the chromophore is specified for the cis-HSD protonation state in Figure 1 and follows the characteristic nomenclature for the atoms in the original amino acid sequence of the BFP.

B. QM/MM Dynamics and Minimizations. The structures were prepared according to the following protocol. The X-ray structure (2.1 Å resolution) of the BFP resolved by Remington et al.[3] (PDB code: 1BFP) was taken as the reference structure. The protein is composed of 238 amino acids, the last nine C terminal residues missing, and corresponds to the Y66H/Y145F variant of the *Aequorea victoria*'s GFP. The protein is folded in a β-sheet barrel conformation, with the chromophore occupying a central position inside the barrel as in the GFP.[5] The chromophore is formed by the sequence Ser65, His66 (which substituted Tyr66 of the wt-GFP), and Gly67. The residue Ser65 is chemically modified so that its carbonyl carbon is linked to the nitrogen of Gly67 and the carbonyl oxygen is eliminated. As a result, the chromophore is formed by two consecutive rings, the imidazole-type ring of His66 and a five-membered heterocycle (imidazolinone) formed by the backbone of His66, the carbonyl carbon of Ser65 and the nitrogen of the backbone of Gly67 (see Figure 1). In the X-ray structure, several water positions were identified, some of them lying inside the β-sheet barrel. These water molecules were kept in the calculations, and water molecules were added to fill empty spaces and to complement a 5 Å solvation shell around the protein.

Departing from these coordinates, the positions of the hydrogen atoms were initially estimated using the HBUILD command[20] of CHARMM.[21] The CHARMM force field and parameters[22] were employed for all of the calculations. An initial geometry optimization was performed with all atoms within 10 Å of the chromopeptide free to move and the rest of the atoms fixed at their crystallographic positions. No cutoff was introduced to treat nonbonded interactions. The system was minimized using the steepest descents and adaptive basis Newton−Raphson minimization algorithms available in CHARMM. After this initial relaxation, a second geometry optimization was performed, allowing this time all atoms to relax.

Since the structure of the chromophore, especially due to the heterocycle, does not correspond to the typical structure adopted by a serine, a histidine, or a glycine, there was a lack of specific force-field parameters. Therefore, we decided to perform these calculations using a quantum mechanical/molecular mechanical hybrid Hamiltonian[23] (QM/MM), with an AM1 semiempirical Hamiltonian[24] to describe the quantum part.[37] The QM region was formed by the Ser65, His66, and Gly67 residues, and the frontier between QM and MM regions was

(18) Becke, A. *J. Chem. Phys.* **1993**, *98*, 5648−5652.
(19) Hehre, W.; Radom, L.; Schleyer, P.; Pople, J. *Ab Initio Molecular Orbital Theory*; Wiley-Interscience: New York, 1986.
(20) Brunger, A.; Karplus, M. *Proteins* **1988**, *4*, 148−156.
(21) Brooks, B. R.; Bruccoleri, R. E.; Olafson, B. D.; States, D. J.; Swaminathan, S.; Karplus, M. *J. Comput. Chem.* **1983**, *4*, 187−217.
(22) MacKerell, A. D., Jr.; Bashford, D.; Bellott, M.; Dunbrack, R. L., Jr.; Evanseck, J. D.; Field, M. J.; Fischer, S.; Gao, J.; Guo, H.; Ha, S.; Joseph-McCarthy, D.; Kuchnir, L.; Kuczera, K.; Lau, F. T. K.; Mattos, C.; Michnick, S.; Ngo, T.; Nguyen, D. T.; Prodhom, B.; Reiher, W. E., III; Roux, B.; Schlenkrich, M.; Smith, J. C.; Stote, R.; Straub, J.; Watanabe, M.; Wiorkiewicz-Kuczera, J.; Yin, D.; Karplus, M. *J. Phys. Chem. B* **1998**, *102*, 3586−3616.
(23) Field, M. J.; Bash, P. A.; Karplus, M. *J. Comput. Chem.* **190**, *11*, 700−733.
(24) Dewar, M.; Zoebisch, E.; Healy, E.; Stewart, J. *J. Am. Chem. Soc.* **1985**, *107*, 3902−3909.
(25) The octopus project is aimed at describing the electron−ion dynamics in finite and extended systems under the influence of time-dependent electromagnetic fields. The program can be freely downloaded from it http://www.tddft.org/programs/octopus. For details, see: Marques, M. A. L.; Castro, A.; Bertsch, G. F.; Rubio, A. *Comput. Phys. Commun.* **2000**, *151*, 60−78.
(26) (a) Yabana, K.; Bertsch, G. F. *Phys. Rev. B* **1996**, *54*, 4484−4487. (b) Yabana, K.; Bertsch, G. F. *Int. J. Quantum Chem.* **1999**, *75*, 55−66.
(27) Castro, A.; Marques, M. A. L.; Alonso, J. A.; Rubio, A. *J. Comput. Theor. Nanoscience* **2004**, *1*, 230−253.
(28) Castro, A.; Marques, M. A. L.; Rubio, A. *J. Chem. Phys.* **2004**, *121*, 3425−3433.

treated within the H-link approximation. In this approach, a hydrogen atom was included whenever the frontier between the QM and MM regions passed through a chemical bond. This H-link atom was forced during the minimization to be in the line along the frontier bond, and it did not interact with the MM atoms. To avoid the QM/MM frontier to be in the C(O)−N peptide bond, the carbonyl group of Gly67 was removed from the QM part and the carbonyl group of Phe64 was included. In this way, the two H-link atoms included cut through C−C bonds. The resultant QM zone is depicted in Figure 1.

In addition, we also minimized the structure following a different protocol, in which a short QM/MM molecular dynamics of 200 ps was carried out at 300 K with 0.5 fs time steps. After this molecular dynamics simulation, the geometry of the BFP was again fully relaxed. The structure thus obtained was very similar to the one obtained with the QM/MM minimization using the X-ray geometry as the starting point.

C. Excitation Energies in TDDFT. At least two different approaches are commonly used within TDDFT to calculate electronic excitations: one based on the direct propagation of the time-dependent Kohn−Sham equations,[8] and the other, more widely used, based on the identification of the pole structure of the linear response function, known as Casida's equations.[9,10] The two are fully equivalent in that one works in the linear response regime when solving the time-dependent Kohn−Sham equations[10−13] (see below).

In the present work, we follow the former, more direct route to compute excitation spectra. The scheme is based on solving in real-space the time-dependent Kohn−Sham equations for a system responding to a perturbing electromagnetic field.[25] This method has been successfully applied to clusters[26,27] and biomolecules.[8,27]

The starting point for the time-dependent simulations is the Kohn−Sham ground state of the electronic system. The time-dependent equation is then solved for the occupied Kohn−Sham orbitals ψ_i in the presence of the (time-dependent) perturbation $\delta v_{\text{ext}}(\boldsymbol{r}, t)$

$$i\hbar\frac{\partial\psi_i(\boldsymbol{r}, t)}{\partial t} = \left[-\frac{\hbar^2}{2m}\nabla^2 + v_{\text{ion}}(\boldsymbol{r}) + v_{\text{Hxc}}(\boldsymbol{r}, t) + \delta v_{\text{ext}}(\boldsymbol{r}, t)\right]\psi_i(\boldsymbol{r}, t) \quad (1)$$

where v_{ion} denotes the potential generated by the nuclei and v_{Hxc} is the Hartree plus exchange-correlation potential.

To obtain the linear optical absorption spectrum, one excites all frequencies of the system by applying the electric field $\delta v_{\text{ext}}(\boldsymbol{r}, t) = -\kappa z\delta(t)$. (This is equivalent to giving a small momentum κ to the electrons.) The Kohn−Sham wave functions at time δt can be obtained analytically and read as $\psi_i(\boldsymbol{r},\delta t) = e^{i\kappa z}\psi_i(\boldsymbol{r}, 0)$. Those orbitals are then propagated in time using a unitary and stable scheme.[28] From the induced density $\delta n(\boldsymbol{r},\omega)$, it is then straightforward to calculate the time-dependent induced dipole moment, from which the photoabsorption cross-section follows

$$\sigma(\omega) = \frac{4\pi\omega}{\kappa c}\mathcal{I}\int d^3r\, v_{\text{ext}}(\boldsymbol{r})\delta n(\boldsymbol{r},\omega) \quad (2)$$

where c is the velocity of light. For small κ, this time evolution maps the linear response of the system, thus being equivalent to solve Casida's equations.[10]

There are several advantages in our method relative to the traditional linear response function approach:[10] (i) the scaling with the number of atoms is more favorable; (ii) we do not need an approximation to the exchange-correlation kernel (only the exchange-correlation *potential* appears during the equations); (iii) only the occupied states need to be propagated, so there is no need to compute empty states; (iv) this method is trivially extended to nonlinear response and is ideal to be combined with molecular simulations of the ions.

All calculations of the BFP chromopeptide were performed with the code octopus.[25] The electron−ion interaction was described using norm-conserving pseudopotentials.[29] All quantities were computed using a uniform grid-spacing of 0.23 Å and a time-step of 0.002 $\hbar$/eV. The time evolution was run for a maximum time of 20 fs, which yielded spectra with a resolution of about 0.1 eV.

Finally, some words on the choice of the approximation to the exchange-correlation potential. We recognize that the LDA functional is less successful than either GGA or hybrid functionals for the purpose of computing both structural and energetic properties.[30] However, it is well-known that using the traditional generalized gradient approximations (GGA) does not lead to significant improvements over the local density approximation (LDA) for the calculation of absorption spectra.[31] Furthermore, the spectra calculated in this way turn out to be in quite good agreement with experimental data, typically with an error of about 0.1 eV.[8,11,12,27] There are, however, some important exceptions to this rule, namely, infinite, periodic systems[13] and charge-transfer processes.[32] With this in mind, we opted for using the LDA in the parametrization of Perdew and Zunger,[33] due to its numerical stability.

III. Results and Discussion

A. Isolated Chromophore. In this section, we study the BFP chromophore in the gas phase. Several structures are considered, involving three different protonation states—anionic (HSA), neutral (HSE or HSD), and cationic (HSP), and three different conformers—the cis, the trans, and the transition state (TS). All of these structures are depicted in Figure 2.

1. Structure and Energetics. For each protonation state of the BFP, there are two stable conformations, a cis and a trans, defined with respect to the relative position of the two nitrogens, N_δ and N_γ, on the imidazole and imidazolinone rings, respec-

(29) (a) Troullier, T.; Martins, J. L. *Phys. Rev. B* **1991**, *43*, 1993−2006. (b) Kleinman, L.; Bylander, D. M. *Phys. Rev. Lett.* **1982**, *48*, 1425−1428. In this work, we used the core radii r_c = 1.49, 1.39, and 1.39 au for the s, p, and d components of the carbon, nitrogen, and oxygen pseudopotentials. The pseudopotentials can be downloaded from the octopus web page.[25]
(30) Mercero, J. M.; Matxain, J. M.; Lopez, X.; York, D. M.; Largo, A.; Eriksson, L. A.; Ugalde, J. M. *Int. J. Mass. Spectrom.* **2005**, *240*, 37−99.
(31) Marques, M. A. L.; Castro, A.; Rubio, A. *J. Chem. Phys.* **2001**, *115*, 3006−3014.
(32) Dreuw, A.; Head-Gordon, M. *J. Am. Chem. Soc.* **2004**, *126*, 4007−4016.
(33) Perdew, J. P.; Zunger, A. *Phys. Rev. B* **1981**, *23*, 5048−5079.
(34) Boyé, S.; Nielsen, I.; Nielsen, S.; Krogh, H.; Lapierre, A.; Pedersen, H.; Pedersen, S.; Pedersen, U.; Andersen, L. *J. Chem. Phys.* **2003**, *119*, 338−345.
(35) Laino, T.; Nifosi, R.; Tozzini, V. *Chem. Phys.* **2004**, *298*, 17−28.
(36) Cui, Q.; Elstner, M.; Kaxiras, E.; Frauenheim, T.; Karplus, M. *J. Phys. Chem. B* **2001**, *105*, 569−585.
(37) The precision of the AM1 semiempirical method for these systems was tested by performing gas-phase calculations for all chromopeptide isomers in the various protonation states and comparing to the B3LYP relative energies. It was found that, for the three protonation states, AM1 and B3LYP gave the same lowest-energy conformer. Thus, the AM1 relative energies (in kcal/mol) for each protonation state are: trans-HSA (−2.3) < cis-HSA (0.0), cis-HSD (−6.7) < trans-HSE (−3.4) < trans-HSD(−2.9) < cis-HSE (0.0), and cis-HSP (−2.3) < trans-HSP (0.0). In addition, there is a very good agreement between the AM1 and B3LYP gas-phase geometries for cis-HSD (the isomer for which we performed extensive QM/MM simulations): $C_\alpha-C_\beta$ distance is 1.350 Å, $C_\beta-C_\gamma$ distance is 1.427 Å, $C_\alpha-C_\beta-C_\gamma$ angle is 126.7°, DH1 is 0.1°, and DH2 is −0.3°.
(38) The main structural features of the AM1/MM calculations were confirmed by two additional geometry minimizations using two other methods. In the first, the SCC−DFTB method[36] interfaced with CHARMM was used, and the system was prepared with the same definitions for the QM and MM regions as in the AM1/MM calculations. In the second method, we performed a full QM calculation using B3LYP/6-31G* but with limiting the definition of the protein environment to the side chain of His148, Glu222, and Arg96. A constrained geometry optimization was then performed with some of the His148, Glu222, and Arg96 side chain atoms fixed at their AM1/MM positions. We found that these two new structures were qualitatively similar to the structure obtained by AM1/MM. In particular, all of them exhibited: (i) $C_\alpha-C_\beta < C_\beta-C_\gamma$, (ii) very small DH1 angles, and (iii) DH2 values that denote an important breakdown of the coplanarity of the two rings in the chromopeptide: −15.6° (SCC−DFTB/MM), −11.4(B3LYP/6-31G*).
(39) Here, we take $\sigma(\omega) = \int d\alpha f(\alpha, T)\sigma(\alpha,\omega)$, where α denotes the DH2 angle, $\sigma(\alpha,\omega) = \sigma_{\text{TS}}(90,\omega) + (1 - \alpha/90)(\sigma_{\text{cis}}(0,\omega) - \sigma_{\text{TS}}(90,\omega)$ is given in terms of the absorption cross-section of the cis and TS conformations.

Table 1. Some Relevant Geometrical Features of the Chromophores Shown in Figure 2[a]

	Distances					Angles		
	C_α–C_β	C_β–C_γ	X	N_β–X	$N_\gamma H_\delta$	C_α–C_β–C_γ	DH1[b]	DH2[b]
				Anionic HSA				
cis	1.383	1.409	N_δ	3.302		133.5	0.0	0.0
TS	1.355	1.469				127.9	0.0	89.2
trans	1.386	1.406	C_δ	3.231	2.737	130.4	0.0	180.0
				Neutral HSE				
cis	1.356	1.441	N_δ	3.171		130.4	0.0	0.0
TS	1.345	1.476				124.9	1.4	83.6
trans	1.357	1.439	C_δ	3.075	2.596	127.1	0.0	180.0
				Neutral HSD				
cis	1.362	1.426	N_δ	2.853	2.165	125.6	0.0	0.0
TS	1.347	1.471				124.8	−1.4	91.8
trans	1.359	1.430	C_δ	3.182	2.687	127.1	0.0	180.0
				Cationic HSP				
cis	1.355	1.441	N_δ	2.696	1.913	122.2	0.0	0.0
TS	1.348	1.469				121.9	−0.8	92.9
trans	1.355	1.438	C_δ	3.013	2.523	123.5	0.0	180.0

[a] Bond distances are in angstroms and angles in degrees. [b] DH1 stands for the dihedral angle formed by the N_γ−C_α−C_β−C_γ nuclei, and DH2 is the dihedral angle formed by N_δ−C_γ−C_β−C_α.

Table 2. Relative Energies in the Gas Phase with Respect to the cis Conformer for the Various Protonation States of the Chromophore[a]

	ΔE_e	ΔE_0	ΔH	$T\Delta S$	ΔG
			Anionic HSA		
cis	0.00	0.00	0.00	0.00	0.00
TS	17.83	17.08	16.80	-0.58	17.38
trans	-3.45	-3.36	-3.37	-0.06	-3.31
			Neutral HSE		
cis	0.00	0.00	0.00	0.00	0.00
TS	5.34	5.05	4.62	-1.08	5.70
trans	-4.76	-4.64	-4.69	-0.23	-4.46
			Neutral HSD		
cis	-10.47	-10.01	-10.17	-0.57	-9.60
TS	4.79	4.59	4.17	-1.00	5.17
trans	-4.74	-4.59	-4.60	-0.10	-4.50
			Cationic HSP		
cis	0.00	0.00	0.00	0.00	0.00
TS	13.70	13.43	13.16	-0.37	13.54
trans	6.28	6.19	6.37	0.61	5.76

[a] For the case of the neutral chromophores, we have selected the cis-HSE as reference. All numbers are in kcal/mol. E_e corresponds to the electronic energy; E_0 corresponds to the electronic energy plus the zero-point vibrational energy correction, H to the enthalpy, T to the temperature, S to the entropy, and G to the free energy.

tively. The transition state connecting them, which corresponds to a torsion around the C_β−C_γ bond was obtained by constrained minimization for each fixed torsion angle. All relevant structural information of the isolated chromophores can be found in Table 1. In all of these structures, irrespective of the total charge of the system and of the conformation, the C_α−C_β bond distance is shorter than that of C_β−C_γ, indicating a larger double bond character for the C_α−C_β bond. As expected, all cis and trans conformers exhibit coplanarity of both imidazole and imidazolinone rings, as indicated by the values of the dihedral angles DH1 (N_γ−C_α−C_β−C_γ) and DH2 (N_δ−C_γ−C_β−C_α). At the transition states, both rings lie in almost perpendicular planes (DH2 varying from 83.6 in TS−HSE to 92.9 in TS−HSP).

The relative energies, with respect to the cis conformer in each protonation state, are shown in Table 2 (for the two neutral species HSE and HSD, we took the cis-HSE as energy reference). Quite interestingly, the nature of the lowest-energy conformer (cis or trans) varies with the protonation state. In the case of the HSA and HSE, the trans conformers are more stable, whereas for the HSD and HSP, the cis conformers are favored. These trends can be explained by simple qualitative arguments: the conformer with a proton closer to the nitrogen of imidazolinone (N_γ) is favored because of a favorable internal hydrogen bond/electrostatic interaction with this proton. In the case of the HSA and HSE, this conformation happens to be the trans. In the case of the HSD and HSP, both cis and trans conformers have a proton located for a favorable interaction with N_γ. However, the cis conformers are favored due to the higher polarity of the N−H bond.

2. Optical Absorption in the Gas Phase. Figure 3 shows the TDDFT optical absorption spectrum for each protonation state and conformation of the chromophore in the gas phase. To help the discussion, we collect in Table 3 the positions of the main peaks for each spectrum. The spectrum is sensitive to both protonation state and conformation of the chromophore.

For the cis-HSD, the lowest-energy chromophore in the neutral state, there are two main peaks in the 2−5 eV region: at 3.24 and 3.82 eV. Isomerization to the trans conformation leaves the first of these peaks almost unaffected. However, the second one is shifted by 0.1 eV and witnesses a significant decrease of its absorption strength. At the TS, and due to the orthogonality of the two rings, the main absorption peaks are shifted to energies higher than 5 eV (5.21 eV), and only low absorption strengths are observed in the 2−5 eV range. These results reveal the important dependence of the optical properties of the chromophore on the relative orientation of the imidazole and imidazolinone rings. In fact, the breaking of planarity going from the cis to the TS makes the evolution of the two lower-energy peaks depend on the protonation state; we get a red-shift for the HSD and HSA chromophores, whereas a blue-shift is obtained for the HSP and HSE. This will have important consequences when discussing the optical properties of the chromopeptide in the protein matrix, where the most likely configurations compatible with X-ray data are the cis-HSD and HSA.

The spectrum is also sensible to the specific tautomer of the neutral chromophore. In cis-HSE, two peaks of almost equal heights at 3.32 and 3.97 eV are obtained and two smaller peaks at 4.42 and 4.65 eV. Isomerization to the trans conformation has a very small influence on the position of the first peak, but the second peak almost disappears. Finally, in the transition state, there is very little absorption between 2 and 5 eV.

The changes in the optical spectrum are more pronounced when we consider the anionic and cationic states of the chromophore. The main absorption peaks for the HSP (cationic state) are located at 4.06 eV for cis and 4.02 eV for trans, significantly higher than for the neutral states. There is a second peak at lower energies, 3.00 eV (cis) and 2.88 eV (trans), but of much lower intensity. However, in the case of the anionic state HSA, the main peaks overlap with the absorption region of the neutral state, the main absorption being at 3.24 eV (cis) and 3.05 eV (trans). This behavior remains unaffected by the protein environment and is relevant for the interpretation of the measured optical spectra of BFP (see discussion below). Note that this characteristic of the anionic spectrum is fundamentally different from the spectrum of the wt-GFP, for which the main

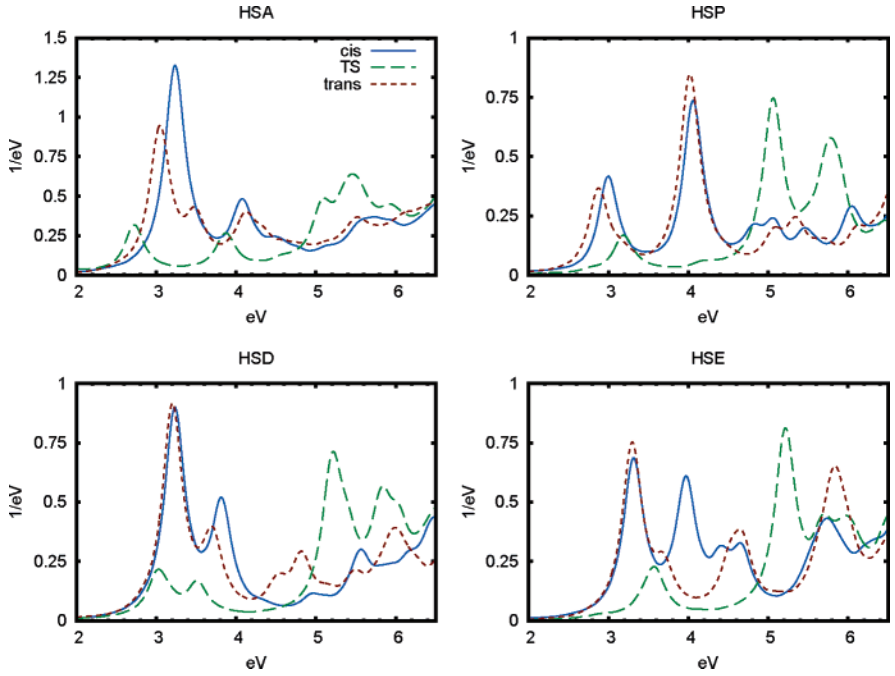

Figure 3. Optical absorption spectrum in the range of 2−5 eV for the various protonation states and conformers of the chromopeptide in the gas phase (cis: blue solid line; TS: green dashed line; and trans: red dotted line). Refer to Figure 2 for details on the geometries.

Table 3. Main Absorption Peaks (with more than 0.5 oscillator strength) of the Chromophore in the Gas Phase Corresponding to Figure 3[a]

	conformation		
protonation state	cis	TS	trans
anionic HSA	3.24	5.46	3.05
neutral HSE	3.32	5.21	3.30
	3.97		
neutral HSD	3.24	5.23	3.20
	3.82		
cationic HSP	4.06	5.06	4.02

[a] All number are given in eV.

absorption peak of the anionic state is 0.4 eV below the neutral state (i.e., 2.63 versus 3.05 eV).[1]

Taking together the absorption maxima for the lowest-energy conformer in each protonation state, we have the following order in absorption energies as a function of the protonation state of the chromopeptide in the gas phase (in eV)

$$3.05(\text{HSA}) < 3.24(\text{HSD}) < 4.06(\text{HSP})$$

This trend is in qualitative agreement with the reported experimental absorption maxima of the chromopeptide in solution,[3] namely (in eV)

$$2.99(\text{anionic}) < 3.38(\text{neutral}) < 3.53(\text{cation})$$

However, whereas the quantitative agreement is quite reasonable for the anionic and neutral states, there is a difference of ∼0.5 eV in the absorption peak of the cationic state. This difference is too high to be ascribed to an error of our computational method and, therefore, points to a significant solvent stabilization of the excited cationic state. In this respect, it has been reported[34] that the cationic state of the chromopeptide of the GFP−Y66W mutant (where a tryptophan ring has been included instead of Tyr66) is sensitive to solvent effects as well, whereas the optical response of its anionic state is almost unchanged in different solvents. Our results can be interpreted in the same way. We remark that the special β-can structure of the BFP provides shielding of the chromopeptide with respect to the aqueous solvent. However, the spectrum of the chromopeptide inside the BFP can be influenced by the interactions with vicinal amino acids and buried water molecules, and by protein-induced conformational changes. This is analyzed in detail in the next section.

B. Chromophore in the Protein Matrix. 1. Structure of the cis-HSD Chromopeptide in the BFP Based on QM/MM Calculations. To study the effect of the protein environment on the structure of the chromopeptide, QM/MM simulations of the chromopeptide embedded inside the BFP were performed. From the several protonation states of the chromophore, we chose to start with the cis-HSD. This choice was motivated by two reasons: (i) this is the lowest-energy structure for the neutral chromophore; and (ii) the X-ray data indicate that the N_δ and the N_γ atoms are in a cis conformation.

In Figure 1, we display the geometry of the chromophore together with its closest residues after the 200 ps MD run followed by a full QM/MM minimization. Selected geometrical parameters can be found in Table 4. The DH1 and DH2 dihedral angles and the $C_\alpha-C_\beta$ and $C_\beta-C_\gamma$ distances, collected along the simulation, are shown in Figure 4. As in the gas phase, we found that during the simulation the values for the $C_\alpha-C_\beta$ distance were smaller than that for $C_\beta-C_\gamma$. More interestingly, the inspection of the DH2 dihedral angle indicates that the relative orientation between the imidazole and imidazolinone planes suffers important changes with respect to the gas-phase structures. While the average value of DH1 is 0.8°, indicating very small torsion around the $C_\alpha-C_\beta$ bond, the DH2 dihedral significantly departs from gas-phase values, with an average value of −18.3°. Thus, the chromopeptide shows a considerable nonplanarity within the protein matrix. Other methods[38] also confirmed the breakdown of planarity of the chromopeptide within the protein, although the AM1 method seems to give

Table 4. Selected Geometrical Parameters of the cis-HSD from the QM/MM Dynamics and Minimizations[a]

	$\langle x \rangle$	x_{min}
DH1	0.8	1.5
DH2	−18.3	−19.6
C_α-C_β	1.350	1.348
C_β-C_γ	1.428	1.427
$N_\epsilon^{His66}-H_{N\epsilon}^{His148}$	1.844	1.809
$H_{N\delta}^{His66}-O_{\epsilon 1}^{Glu222}$	2.508	2.318
$H_{N\delta}^{His66}-O_{\epsilon 2}^{Glu222}$	1.957	1.997

[a] The values of $\langle x \rangle$ and x_{min} differ since the potential around the minimum-energy dihedral angle is not symmetrical.

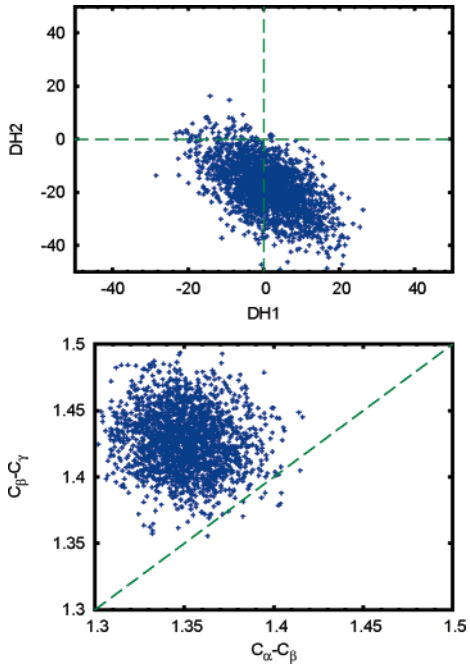

Figure 4. (Top) DH1 ($N_\gamma-C_\alpha-C_\beta-C_\gamma$) versus DH2 ($N_\delta-C_\gamma-C_\beta-C_\alpha$) dihedral angles collected along the QM/MM dynamics of the chromopeptide in the BFP. (Bottom) $C_\alpha-C_\beta$ distance versus $C_\beta-C_\gamma$ along the QM/MM dynamics.

the maximum degree of nonplanarity among the tested methods. Hence, the results presented in this section should be taken as the maximum effect expected from a likely chromopeptide distortion. The torsion around the $C_\beta-C_\gamma$ bond optimizes the orientation of $H_{N\delta}^{His66}$ for a hydrogen bond interaction with the negatively charged Glu222. The average $H_{N\delta}^{His66}-O_{\epsilon 2}^{Glu222}$ distance is 1.957 Å, and after full optimization, 1.997 Å—typical values for a hydrogen bond. This departure of the planarity is energetically possible since the $C_\beta-C_\gamma$ bond has a considerable smaller double bond character than the $C_\alpha-C_\beta$ bond.

2. Optical Spectrum of the Neutral cis-HSD. To determine the role played by the protein intramedia in the optical spectroscopic properties of the chromopeptide, we selected various structures from the QM/MM minimization of the BFP and performed TDDFT calculations. The results can be found in Table 5 and in Figure 5. In Figure 5, we compare the experimental absorption spectrum with the gas-phase spectrum, the optical spectrum of the chromopeptide with the geometry adopted inside the BFP protein (i.e., a DH2 of −19.6° at the QM/MM minimized structure), and the spectrum of the chromopeptide plus a selection of some of the closest residues around

Table 5. Absorption Energies in the Spectrum of the cis-HSD and cis-HSA Chromophores in Different Configurations: Gas Phase and Distorted as Inside the Protein (including different local environments)[a]

Structure	Environment	Peaks	
Experiment			
		3.21	
		(3.05, 3.36)	
Neutral cis-HSD			
planar	gas phase	3.24	3.82
distorted		3.09	3.54
distorted	Env. I	3.04	3.39
distorted	Env. II	3.08	3.48
Anionic cis-HSA			
planar	gas phase	3.24	
distorted		3.10	
distorted	Env. I	3.04	
distorted	Env. II	3.08	

[a] Only the peaks with an absorption larger than 0.5 in the range between 2 and 5 eV are shown. The experiment has a main peak at 3.21 eV with two shoulders that are also given in parentheses.

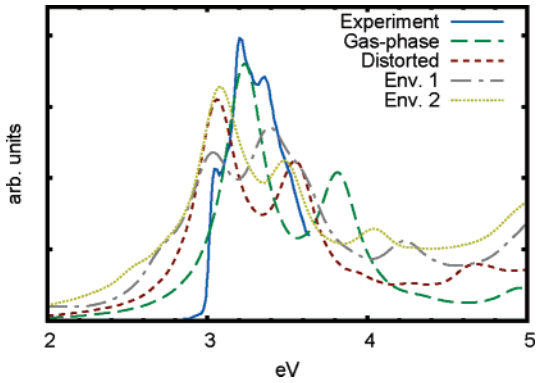

Figure 5. Optical absorption spectrum for the cis-HSD state of the chromophore in the gas phase and distorted by the BFP protein environment, compared with the experimental spectrum of the BFP.

the chromophore, which we named the *environment* of the chromophore. We have studied two different environments (see Figure 1). (i) Env. I includes His148, Glu222, and Arg96, which are the charged residues in the vicinity of the chromophore (His148 and Arg96 positive; Glu222 negative). As such, it is reasonable to expect that they will have a greater influence in polarizing the electronic cloud of the chromopeptide. (ii) Env. II is composed by Env. I to which we add Ser205, a buried water molecule, and Gln94. All of these are polar residues that are within 2.5 Å of the chromophore.

The induced nonplanarity in the chromopeptide by the protein environment has a sizable effect in the spectrum. It causes a considerable red-shift of the gas-phase cis-HSD peaks, from 3.24 to 3.09 eV and from 3.82 to 3.54 eV. Thus, the optical absorption is sensitive to the ∼20° torsion around the $C_\beta-C_\gamma$ bond of the chromopeptide. Quite interestingly, similar distortions have been found for the neutral state of the chromopeptide in the wt-GFP, and these distortions also affect in a similar way the spectrum of the GFP.[8,35]

On the other hand, the effect of the polarization of the electronic cloud by neighbor residues is less important. The inclusion of the residues His148, Glu222, and Arg96 in the calculations (Env. I) causes a further red-shift of the second peak to 3.39 eV, but leaves the first peak (which is the absorption maximum) almost unchanged at 3.04 eV. However,

when enlarging the environment to Env. II, we find a spectrum with a shape similar to the one of the twisted chromopeptide with two well-defined peaks at similar positions, 3.08 and 3.48 eV. It seems that in our calculations, Env. I provides an inhomogeneous surrounding to the chromopeptide, which leads to an over-polarization of the electronic cloud. This artifact is corrected when the chromophore is equally surrounded in all directions. This delicate cancellation of the shielding of the applied electromagnetic field is important when defining the structure used for the calculation of the linear response.

In summary, the calculations of the optical absorption of the chromopeptide inside the BFP exhibit a red-shift of the spectrum, which has mainly a structural origin (breakdown of the planarity), with small contributions from polarization effects of the environment. Similar conclusions were reached in the study of the wt-GFP chromophore.[8] The calculated 0.15 eV red-shift provoked by the nonplanarity of the chromopeptide is in quite good agreement with the observed red-shift of 0.13 eV between the unfolded and folded proteins. However, the experimental and theoretical main absorption peaks still differ by 0.17 eV. This difference, although small, can be due to different aspects: (i) errors induced by the use of the local-density approximation to handle exchange-correlation effects; (ii) contribution from different protonation states; (iii) temperature-induced local fluctuations of the chromopeptide; and (iv) errors in the calculation of the exact degree of distortion of the chromopeptide with the AM1/MM Hamiltonian.

3. Other Protonation States. We repeated the calculations of the previous section for other possible protonation states of the chromopeptide. We only mention here the most interesting cases.

Since the pK_a[1] of the chromopeptide is around 4 in solution, one could think that the cationic state is a possible protonation state of the chromopeptide. This is true, especially since the presence of the negatively charged Glu222 can probably shift the pK_a[1] to even higher values. Calculations were, therefore, prepared for this cationic state by putting His148 in its neutral state. The resultant QM/MM dynamics/minimization led again to a nonplanar structure of the chromopeptide but with a DH2 of $-11.9°$. TDDFT calculations of this structure showed an absorption maximum at 3.78 eV, significantly red-shifted with respect to the 4.06 eV of the gas phase. Inclusion of Env. I in the calculations led to a further red-shift, but of smaller degree, yielding 3.70 eV. These values are around 0.5 eV higher than the experimental absorption maximum and, therefore, indicate that this cationic state is not contributing to the observed optical properties in the BFP.

The already mentioned pK_a analysis seems to indicate that the anionic state of the BFP is not present in the ground state of the chromopeptide.[3] However, two reasons led us to investigate further this state: (i) its gas-phase absorption peak is well within experimental range; and (ii) we could think of the anionic state as a result of the deprotonation of the neutral cis-HSD state in the excited state (as it is the case for the neutral state of the GFP), and formation of a protonated Glu222. In order for this state to be sufficiently long-lived, it would require a neutral state for the His148. Thus, we prepared the cis-HSA state of the chromopeptide with His148 in its HSϵ neutral state and Glu222 protonated (neutral charge). The cis-HSA state in the BFP protein environment showed a smaller deviation from

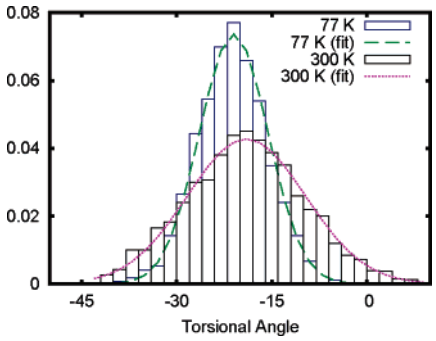

Figure 6. Distribution of DH2 angles from the molecular dynamics simulation.

planarity as compared to the cis-HSD state ($-12°$ versus the $-18.3°$ of the neutral cis-HSD). The spectra consist of a main peak at 3.08 eV with a shoulder at 3.33 eV and a higher energy peak at about 4 eV. The main absorption peak is indistinguishable from the main peak of the cis-HSD conformation. In contrast to the results of the wt-GFP, where the anionic and neutral states are clearly associated to each of the two main absorption peaks, the spectra of the BFP by itself cannot distinguish between the anionic and neutral states.

Still, by looking at the gas-phase data, we conclude that the other neutral state (HSE), although energetically less stable, could also be present in the BFP. Furthermore, the main absorption peak of the gas-phase spectra of HSE is blue-shifted by only 0.1 eV with respect to the more stable HSD conformation. We have investigated the cis-HSE conformation, having the His148 in its neutral HSD state and the Glu222 protonated. We can think of this structure as generated from cis-HSD by protonation of Glu222 by the proton at N_δ of cis-HSD, and in turn, protonation of N_ϵ by His148. Notice that the cis-HSE structure would be also consistent with the X-ray data in that N_δ and N_γ atoms maintain a cis conformation. Thus, although in gas phase the trans-HSE is the minimum of energy, this conformation is very unlikely in the protein environment.

The spectrum consists of two main absorption peaks at 2.83 and 3.56 eV, which are in less agreement with experiments than the spectra obtained with the cis-HSD state of the chromophore. It is remarkable that the red-shift induced by the protein environment is stronger for the HSE than for the HSD state, reversing the order of the main absorption peaks from the gas-phase results. This indicates the importance of treating properly the environment in the calculation of the optical spectra.

From this discussion, it seems that the cis-HSD is the main contributor to the experimental optical spectrum of the BFP. However, the anionic cis-HSA could also be present in the excited state.

4. Temperature Effects. In the wt-GFP, we know that as we reduce the temperature from 298 to 77 K, the lower-energy peak (resulting from the anionic state) shifts to higher energies, whereas the high-energy peak moves to lower energies.[6] We expect some similar effect to be present in the BFP spectra (note that the experimental measure was done at 77 K[4]). A simple explanation for this shift can be given in terms of the floppy torsional motion of the imida rings in the case of BFP. By inspecting the gas-phase calculations shown in Figure 3, we clearly see that going from the cis to the transition state leads to a shift to lower energies of the two first peaks of the HSD and HSA chromophores.

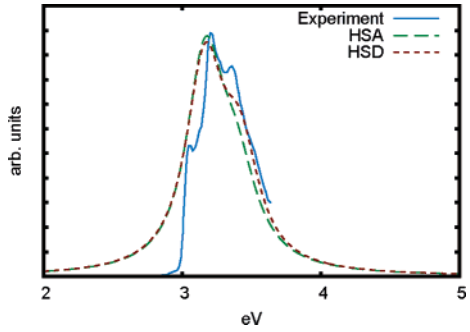

Figure 7. Final comparison between the calculated optical absorption spectra at 77 K for the cis-HSA and HSD states and experiment.

At $T = 0$ K, the protein environment induces a rotation of $-19.6(12)°$ for the neutral (anionic) conformations. To assess the importance of temperature, we performed a constant T molecular dynamics simulation of the neutral HSA conformation. We observed that the chromophore fluctuates quite a lot, mainly in what concerns the DH2 dihedral angle (see Figure 4). A simple model of the optical spectra at finite temperature can be obtained by considering the distribution function of the DH2 angles in the simulation, shown in Figure 6, and assuming that the spectra for a given dihedral angle can be obtained by a linear interpolation between the gas-phase spectra for the cis and the TS (0 and 90°, respectively).[3] If we follow this procedure using the gas-phase data, we realize that the main absorption peak shifts by about 0.1 eV for both the cis-HSA and HSD states. The main peak now occurs at 3.18 eV, in very good agreement with the measured value of 3.21 eV.[4] We can follow the same protocol for the case of the chromophore inside the protein. If we do so, we get the final results of Figure 7. Moreover, we witness an additional blue-shift when going from 80 K to room temperature. The very good agreement with experiment should be taken with some care, as the model used to treat temperature effects is very crude, and more work is needed in order to properly include temperature effects into the optical absorption spectra. However, the present model serves to illustrate the role of the temperature in the final spectra of the BFP.

Conclusions

In this work, we studied the excitation properties of the BFP to disentangle which protonation states are present in vivo. The main candidate turns out to be a neutral cis configuration. However, in contrast to the wt-GFP, where anionic and neutral states yield a distinct peak structure that is responsible for the double peak in the optical spectra,[1,6,8] in the BFP, both anionic and neutral configurations have very similar spectra. There are only minor differences in the fine structure close to the main peak (a shoulder in the HSA is not present in the HSD), while the major differences occur only at much higher photon absorption energies. Therefore, from the optical analysis, we cannot rule out the formation of the anionic HSA configuration in the excited state. Furthermore, other protonation states (such as the positive HSP conformer) cannot be present in the BFP protein as their spectral features are outside the measured absorption spectra.

We have shown the importance of including the protein-induced structural changes of the chromophore. This mainly translates into the breaking of planarity of the otherwise planar gas-phase structures. Our calculations suggest that this breakdown of planarity could be responsible for the 0.13 eV red-shift observed between folded and unfolded conformations of the BFP protein.[3] Furthermore, our calculations show a subtle cancellation of the shielding of the electromagnetic field acting on the chromophore due to its closest residues. This cancellation effect shows that the calculated spectra for the isolated (twisted) chromophore and that for the chromophore in the protein are nearly identical.

Another important conclusion regards the importance of temperature-induced fluctuations of the angle between the two imida rings. Once this effect is taken into account, we get an additional 0.1 eV blue-shift of the spectra, which brings the calculated spectrum in very good quantitative agreement with experiment. Furthermore, this effect might also be the reason for the small difference between the measured and calculated neutral conformation of the wt-GFP in our previous calculations.[8] Still, we do not reproduce the fine structure of the spectra, which can be caused by vibrational sidebands. These effects are, however, beyond the goal of the present study.

In conclusion, we were able to reproduce the measured spectrum of the BFP with high accuracy, and we were able to identify which protonation state of the chromophore is most likely. These results, together with our previous work on the wt-GFP, confirm the predictive capabilities of our QM/MM−TDDFT approach. However, we still lack a complete understanding of the excited-state dynamics of protein chromophores. To have a proper description of those systems would require an extension of the present QM/MM techniques to allow for a better description of the environment excitations and the structural transformations in the excited state. Work along those lines is already in progress.

Acknowledgment. This research was funded by Euskal Herriko Unibertsitatea (the University of the Basque Country), Gipuzkoako Foru Aldundia (the Provincial Government of Guipuzkoa), and Eusko Jaurlaritza (the Basque Government). A.R. and M.A.L.M. were also supported by the European Community 6th framework Network of Excellence NANO-QUANTA (NMP4-CT-2004-500198). Some of the computations were performed in the Laboratório de Computação Avançada of the University of Coimbra (Portugal). A.R. acknowledges the Humboldt Foundation under the Bessel research award (2005).

Supporting Information Available: Complete ref 14. Discussion on the reliability of the QM/MM model based on the semiempirical AM1 Hamiltonian for the QM part. This material is available free of charge via the Internet at http://pubs.acs.org.

JA050935L